Research Article

New insight into gyrotactic microorganisms for bio-thermal convection of Prandtl nanofluid over a stretching/shrinking permeable sheet

Kh. S. Mekheimer[1] · **Shaimaa F. Ramadan**[2]

Received: 7 November 2019 / Accepted: 23 January 2020 / Published online: 19 February 2020

Abstract
The use of nanoparticles, has become increasingly utilized for medical applications and is of great interest as an approach to killing or reducing the activity of numerous microorganisms. The motivation of the present study is to scrutinize the impacts of magnetic field, radiation and chemical reaction on non-Newtonian Prandtl fluid containing gyrotactic microorganisms and nanoparticles. The governing nonlinear partial differential equations are decreased to nonlinear ordinary differential equations using appropriate similarity transformation. Our system of equations are solved numerically by using Rung–Kutta–Merson method with Newton iteration in a shooting and matching technique. The impacts of various parameters on velocity, temperature, nanoparticles concentration and density of motile microorganisms for suction ($f_w > 0$), injection ($f_w < 0$) and the case of impermeable plate surface ($f_w = 0$) have been made.

Keywords Porous · Microorganisms · Nanoparticles · Stretching · Shrinking · Suction · Injection · Radiation

1 Introduction

Bioconvection is an entrancing wonder of liquid mechanics that is driven by the swimming movement of microorganisms and has been viewed quite a few years back. Bioconvection designs, which are an aggregate wonder, generally show up due to upswimming of microorganisms that are denser than water in suspensions. At the point when the upper surface of the suspensions ends up being unnecessarily thick a result of gathering microorganisms, it ends up flimsy and microorganisms land down to cause bioconvection. There are some significant similarities and dissimilarities among nanoparticles and motile microorganisms. The motile microorganisms are self-moved which increment the thickness of the base liquid by swimming in a specific heading in the liquid in light of such updates as gravity, light, or substance fascination. Then again nanoparticles are not self-impelled. These nanoparticles are move as a result of such ponders as Brownian development and thermophoresis and are passed on by the movement of the base fluid. A unique idea for structure of bleeding edge microsystems is to solidify a nanofluid with bioconvection. The extension of gyrotactic microorganisms into the nanofluid grows its solidness as a suspension. Bioconvection has various applications in normal systems and biotechnology. Microorganism particles have extensively used to make mechanical and business things like ethanol, bio fuel produced using waste and composts. They are additionally utilized in water treatment plants. Hydrogen gas and biodiesel, a promising sustainable power source are delivered by those microorganisms.

The slip impacts on bioconvection of nanofluid flow with gyrotactic microorganisms and nanoparticles was examined by Tausif et al. [1]. Nanofluid bioconvection

✉ Shaimaa F. Ramadan, shaimaafathey2012@azhar.edu.eg; Kh. S. Mekheimer, kh_mekheimer@yahoo.com | [1]Department of Mathematics, Faculty of Science (Mens), Al-Azhar University, Nasr-City, Cairo, Egypt. [2]Department of Mathematics, Faculty of Science (Girls), Al-Azhar University, Nasr-City, Cairo, Egypt.

SN Applied Sciences (2020) 2:450 | https://doi.org/10.1007/s42452-020-2105-9

containing gyrotactic microorganisms and the impact of chemical reaction in a permeable medium was contemplated by Das et al. [2].The numerical study of heat transfer and Hall current impact on peristaltic propulsion of particle–fluid suspension with compliant wall properties was discussed by Bhatti et al. [3]. Waqas et al. [4] investigated the thermally developed Falkner–Skan bioconvection flow of a magnetized nanofluid in the presence of a motile gyrotactic microorganism: Buongiorno's nanofluid model. The partition of energies for the backward in time problem of thermoelastic materials with a dipolar structure was examined by Marin et al. [5]. Analysis on the bioconvection flow of modified second-grade nanofluid containing gyrotactic microorganisms and nanoparticles was explored by Waqas et al. [6]. The beginning of bioconvection in nanofluid in nearness of gyrotactic microorganisms and nanoparticles saturating a non-Darcian permeable medium was conveyed by Sarkar et al. [7]. Khan et al. [8] reported the convection in gravity-driven thin film non-Newtonian nanofluids flow containing gyrotactic microorganisms. The effect of the nonlinear thermal radiation and gyrotactic microorganisms on the Magneto-Burgers nanofluid was analyzed by Khan et al. [9]. Mahdy [10] explored the gyrotactic microorganisms mixed convection nanofluid flow along an isothermal vertical wedge in porous media. Raju et al. [11] researched the radiative flow of Casson fluid over a moving wedge loaded up with gyrotactic microorganisms.

The work on magnetohydrodynamic has increased sizeable enthusiasm concerning specialists and researchers because of the reality of its changed applications in engineering, biological sciences and physics. It is used to heat, pump, stir and levitate liquid metals. The static magnetic field is used for the laminarization of contactless damping violent stream in the for-mation of semiconductor precious stones or the consistent throwing of steel. What's more, because of the rate of cooling is fundamental for the nature of an item, in this way magnetohydrodynamic is utilized in various assembling strategies to deal with the rate of cooling. The nearness of the nanoparticles upgrades the electrical conductivity property of nanofluids, henceforth making them progressively helpless to the influence of the magnetic field as compared to the conventional base fluids.

Mutuku et al. [12] examined the hydromagnetic bioconvection of nanofluid over a porous vertical plate under the effect of the gyrotactic microorganisms. Alsaedi et al. [13] observed the magnetohydrodynamic (MHD) stratified bioconvective flow of nanofluid due to gyrotactic microorganisms. Mekheimer et al. [14] investigated the peristaltically flow due to a surface acoustic wavy moving wall. Ramzan et al. [15] introduced the impact of radiative magnetohydrodynamic nanofluid flow due to gyrotactic microorganisms with chemical reaction and non-linear thermal radiation. Eldabe and Ramadan [16] discussed the impacts of wall properties, heat absorption and chemical reeaction on peristaltic flow of Rivlin–Ericksen fluid through porous medium. The peristaltically induced MHD slip flow in a porous medium due to a surface acoustic wavy wall was analyzed by Mekheimer et al. [17].

In the present examination we studied the effects of radiation, chemical reaction and magnetic field on the progression of Prandtl fluid containing gyrotactic microorganisms and nanoparticles through permeable medium. In the part of mathematical formulation, our model is formulated by using appropriate similarity transformation and deriving the governing equations. In the part of numerical solution, our system is solved numerically by using Rung–Kutta–Merson method with Newton iteration in a shooting and matching technique. Then, we discuss the impacts of the issue parameters on these arrangements and cleared graphically.

2 Mathematical formulation

A movement of two dimensional, time independent and incompressible non-Newtonian nanofluid containing gyrotactic microorganisms past a penetrable vertical plate through porous medium is considered. The flow is liable to a uniform transvers magnetic field of strength B_o. There is no connected voltage and the magnetic Reynolds number is little, subsequently the prompted magnetic field and Hall impacts are inconsequential. The presence of nanoparticles is acknowledged to have no effect on the direction of microorganisms swimming and on their swimming velocity (Fig. 1).

The constitute equation for Prandtl fluid is given by Akbar [18]:

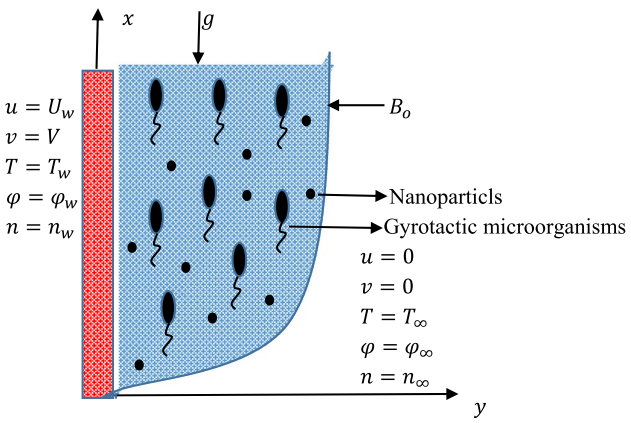

Fig. 1 Geometry of the physical model and coordinate system

$$\tau = \frac{A\ \sin^{-1}\left(\frac{1}{C_1}\left[\left(\frac{\partial u}{\partial y}\right)^2+\left(\frac{\partial v}{\partial x}\right)^2\right]^{\frac{1}{2}}\right)}{\left[\left(\frac{\partial u}{\partial y}\right)^2+\left(\frac{\partial v}{\partial x}\right)^2\right]^{\frac{1}{2}}}\frac{\partial u}{\partial y} \tag{1}$$

where A and C_1 are the material constants of the Prandtl fluid model.

In view of such consideration, the continuity, momentum, energy, nanoparticle concentration and conservation for microorganisms, the equations are:

$$\frac{\partial u}{\partial x}+\frac{\partial v}{\partial y}=0 \tag{2}$$

$$\rho_f\left(u\frac{\partial u}{\partial x}+v\frac{\partial u}{\partial y}\right)=\frac{\partial \tau_{xx}}{\partial x}+\frac{\partial \tau_{xy}}{\partial y}-\left(\frac{\mu}{k}+\sigma B_o^2\right)u+\rho_f g\beta\left(1-\varphi_\infty\right)\left(T-T_\infty\right) - g\left(\rho_p-\rho_f\right)\left(\varphi-\varphi_\infty\right)-g\gamma\left(\rho_m-\rho_f\right)\left(n-n_\infty\right) \tag{3}$$

$$(\rho c)_f\left(u\frac{\partial T}{\partial x}+v\frac{\partial T}{\partial y}\right)=k_T\left(\frac{\partial^2 T}{\partial x^2}+\frac{\partial^2 T}{\partial y^2}\right)+(\rho c)_p\left(D_B\left(\frac{\partial \varphi}{\partial x}\frac{\partial T}{\partial x}+\frac{\partial \varphi}{\partial y}\frac{\partial T}{\partial y}\right)+\frac{D_T}{T_\infty}\left(\left(\frac{\partial T}{\partial x}\right)^2+\left(\frac{\partial T}{\partial y}\right)^2\right)\right) + \left(\tau_{xx}\frac{\partial u}{\partial x}+\tau_{xy}\frac{\partial u}{\partial y}+\tau_{yy}\frac{\partial v}{\partial y}\right)+\sigma B_o^2 u^2-\frac{\partial q_r}{\partial y} \tag{4}$$

$$\left(u\frac{\partial \varphi}{\partial x}+v\frac{\partial \varphi}{\partial y}\right)=D_B\left(\frac{\partial^2 \varphi}{\partial x^2}+\frac{\partial^2 \varphi}{\partial y^2}\right)+\frac{D_T}{T_\infty}\left(\frac{\partial^2 T}{\partial x^2}+\frac{\partial^2 T}{\partial y^2}\right)-k_1\left(\varphi-\varphi_\infty\right) \tag{5}$$

$$u\frac{\partial n}{\partial x}+v\frac{\partial n}{\partial y}+\frac{bW_c}{\left(\varphi_w-\varphi_\infty\right)}\left(\frac{\partial}{\partial y}\left(n\frac{\partial \varphi}{\partial y}\right)+\frac{\partial}{\partial x}\left(n\frac{\partial \varphi}{\partial x}\right)\right)=D_m\left(\frac{\partial^2 n}{\partial x^2}+\frac{\partial^2 n}{\partial y^2}+2\frac{\partial^2 n}{\partial x\partial y}\right) \tag{6}$$

where u and v are velocity component, ρ_f is the density of the fluid, μ is the viscosity, k is the permeability of porous medium, σ is the Conductivity of the fluid, g is the gravity, β is the volume expansion coefficient of the fluid, γ is the average volume of a microorganism, ρ_m is the microorganisms density, $(\rho c)_f$ is the heat capacity of the fluid, $(\rho c)_p$ is the heat capacity of the nanoparticle material, k_T is the thermal conductivity, D_B is the Brownian diffusion coefficient, D_T is the thermophoretic coeffecient, k_1 is the chemical reaction parameter, T is the local temperature, φ is the nanoparticle volume fraction, n is the concentration of the microorganisms, b is the chemotaxis constant, W_c is the maximum cell swimming speed, D_m is the diffusivity of microorganisms.

Using Rosselands approximation [19] for radiative heat flux q_r we have:

$$q_r=-\frac{16\sigma^* T_m^3}{3k^*}\frac{\partial T}{\partial y}, \tag{7}$$

where T_m, σ^* and k^* represent the mean temperature, Stefan Boltzmann and Rosseland mean absorption coefficients. Thus the proper physical conditions near the boundary region as wall as at the distant field may be written as follows:

$$\begin{aligned} &u=U_w,\quad v=V,\quad T=T_w,\quad \varphi=\varphi_w,\quad n=n_w\ at\ y=0,\\ &u\to 0,\quad v\to 0,\quad T\to T_\infty,\quad \varphi\to\varphi_\infty,\quad n\to n_\infty\ at\ y\to\infty, \end{aligned} \tag{8}$$

where T_w, φ_w, n_w are the temperature, nanoparticle volume fraction and density of the motile microorganism at the plate surface. The analogous periphery values are denoted respectively through $T_\infty, \varphi_\infty, n_\infty$. Following [8] the free stream velocity and the suction/injection velocity are assumed to be:

$$U_w=ax\ \text{and}\ V=-\sqrt{av}f_w, \tag{9}$$

where $a>0$ is the initial stretching rate, $f_w>0$ represents suction, $f_w<0$ corresponds to injection and $f_w=0$ is the case of impermeable plate surface, ν is the kinematic viscosity.

Let us introduce the following dimensionless variables and quantities as:

$$\begin{aligned} &\eta=y\sqrt{\frac{a}{\nu}},\quad \psi=\sqrt{a\nu}xf(\eta),\quad \theta(\eta)=\frac{T-T_\infty}{T_w-T_\infty},\\ &\xi(\eta)=\frac{\varphi-\varphi_\infty}{\varphi_w-\varphi_\infty},\quad \chi(\eta)=\frac{n-n_\infty}{n_w-n_\infty}, \end{aligned} \tag{10}$$

where η is the similarity variable and ψ is the stream function which defined as:

$$u = \frac{\partial \psi}{\partial y} \text{ and } v = -\frac{\partial \psi}{\partial x} \tag{11}$$

Substituting from Eqs. (1), (10) and (11) into Eqs. (2)–(9), we obtain the following system of similarity equations:

$$\left(A_2 + A_3\left(f''\right)^2\right)f''' - \left(f'\right)^2 + ff'' - \left(\varepsilon_1 + H_a\right)f' + G_r\left(\theta - N_r\xi - R_b\chi\right) = 0 \tag{12}$$

$$\left(1 + P_rR_n\right)\theta'' + \left(P_rf + N_b\xi'\right)\theta' + N_t\left(\theta'\right)^2 + A_2E_cP_r\left(f''\right)^2 + A_3E_cP_r\left(f''\right)^4 + H_aE_cP_r\left(f'\right)^2 = 0 \tag{13}$$

$$\xi'' + L_ef\xi' + \frac{N_t}{N_b}\theta'' - k_r\xi = 0 \tag{14}$$

$$\chi'' + L_bf\chi' - P_e\left(\xi''(\chi + \Omega) + \chi'\xi'\right) = 0 \tag{15}$$

Subject to the boundary conditions:

$$f(0) = f_w, \quad f'(0) = 1, \quad \theta(0) = 1, \quad \xi(0) = 1, \quad \chi(0) = 1. \tag{16}$$

$$f'(\infty) = 0, \quad \theta(\infty) = 0, \quad \xi(\infty) = 0, \quad \chi(\infty) = 0. \tag{17}$$

where the primes denotes the differentiation with respect to η and A_2, A_3 are Prandtl parameters, ε_1 is porous parameter, H_a is Hartmann number, G_r is Grashof number, N_r is buoyancy ratio parameter, R_b is bioconvection Rayleigh number, P_r is Prandtl number, N_b is Brownian motion parameter, N_t is thermophoresis parameter, E_c is Eckert number, R_n is radiation parameter, L_e is traditional Lewis number, k_r is chemical reaction parameter, L_b is bioconvection Lewis number, P_e is bioconvection Peclet number, Ω is microorganismis concentration difference parameter and f_w is suction/injection parameter. These parameters are defined as:

$$A_2 = \frac{A}{C_1\rho_f\nu}, \quad A_3 = \frac{AaU_w^2}{2C_1\rho_f\nu^2}, \quad \epsilon = \frac{\mu}{a\rho_fk}, \quad H_a = \frac{\sigma B_o^2}{a\rho_f}, \quad G_r = \frac{g\beta\left(1-\varphi_\infty\right)\left(T_w - T_\infty\right)}{aU_w},$$
$$N_r = \frac{\left(\rho_p - \rho_f\right)\left(n_w - n_\infty\right)}{\beta\rho_f\left(1-\varphi_\infty\right)\left(T_w - T_\infty\right)}, \quad R_b = \frac{\gamma\left(\rho_m - \rho_f\right)\left(\varphi_w - \varphi_\infty\right)}{\beta\rho_f\left(1-\varphi_\infty\right)\left(T_w - T_\infty\right)}, \quad P_r = \frac{\nu(\rho c)_f}{k_T},$$
$$N_b = \frac{(\rho c)_pD_B\left(\varphi_w - \varphi_\infty\right)}{k_T}, \quad N_t = \frac{(\rho c)_pD_T\left(T_w - T_\infty\right)}{k_TT_\infty}, \quad R_n = \frac{16\sigma^*T_m^3}{3k^*\nu(\rho c)_f},$$
$$E_c = \frac{U_w^2}{c_f\left(T_w - T_\infty\right)}, \quad L_e = \frac{\nu}{D_B}, \quad k_r = \frac{\nu k_1}{aD_B}, \quad L_b = \frac{\nu}{D_m}, \quad P_e = \frac{bW_c}{D_m}, \quad \Omega = \frac{n_\infty}{n_w - n_\infty}. \tag{18}$$

The parameters wherein we are intrigued for our concern are the skin friction C_f, Nusselt number Nu, Sherwood number Sh and the density number of the motile microorganisms represented by:

$$C_f = \frac{\tau_w}{\rho_fU_w^2}, \quad Nu = \frac{xq_w}{k_T\left(T_w - T_\infty\right)},$$
$$Sh = \frac{xq_m}{D_B\left(\varphi_w - \varphi_\infty\right)}, \quad Nn = \frac{xq_n}{D_n\left(n_w - n_\infty\right)}, \tag{19}$$

where τ_w is the skin friction, q_w is the heat flux, q_m is the surface mass flux and q_m is the surface motile microorganisms flux defined by:

$$\tau_w = \mu\left.\frac{\partial u}{\partial y}\right|_{y=0}, \quad q_w = -k_T\left.\frac{\partial T}{\partial y}\right|_{y=0},$$
$$q_m = -D_B\left.\frac{\partial \varphi}{\partial y}\right|_{y=0}, \quad q_n = -D_n\left.\frac{\partial n}{\partial y}\right|_{y=0} \tag{20}$$

After substituting from (19) in (18) we obtain:

$$C_{fx} = Re_x^{1/2}C_f = f''(0),$$
$$Nu_x = Re_x^{-1/2}Nu = -\theta'(0),$$
$$Sh_x = Re_x^{-1/2}Sh = -\xi'(0),$$
$$Nn_x = Re_x^{-1/2}Nn = -\chi'(0),$$

which are the local skin friction C_{fx}, local Nusselt number Nu_x, local Sherwood number Sh_x, the density number of the motile microorganisms Nn_x and $Re_x = \frac{U_wx}{\nu}$ is the Reynolds.

3 Numerical solution

The system of our nonlinear ordinary differential Eqs. (12–17) is solved by the numerical method based on Rung–Kutta–Merson method with Newton iteration in a shooting and matching technique. To apply shooting method, we use the subroutine D02HAF from the NAG

Fortran library, which requires the supply of starting values of the missing initial and terminal conditions. The subroutine uses Rung–Kutta–Merson method with variable step size in order to control the local truncation error, then it applies modified Newton–Raphson technique mentioned before to make successive corrections to the estimated boundary values. Use the following transformations:

$$f = Y_1, \quad \theta = Y_4, \quad \xi = Y_6, \quad \chi = Y_8$$

Equations (12)–(15) with the boundary conditions (16) and (17) can be written as follows:

$$Y_1' = Y_2, \quad Y_2' = Y_3, \quad \left(A_2 + A_3 Y_3\right) Y_3' = \left(Y_2\right)^2 - Y_1 Y_3 + \left(\epsilon + H_a\right) Y_2 - G_r\left(Y_4 - N_r Y_6 - R_b Y_8\right) \tag{21}$$

$$Y_4' = Y_5, \quad \left(1 + P_r R_n\right) Y_5' = -\left(P_r Y_1 + N_b Y_7\right) Y_5 - N_t \left(Y_5\right)^2 - A_2 E_c P_r \left(Y_3\right)^2 - A_3 E_c P_r \left(Y_3\right)^4 - H_a E_c P_r \left(Y_2\right)^2 \tag{22}$$

$$Y_6' = Y_7, \quad Y_7' = -L_e Y_1 Y_7 - \frac{N_t}{N_b} Y_5' + k_{r1} Y_6 \tag{23}$$

$$Y_8' = Y_9, \quad Y_9' = -L_b Y_1 Y_9 + P_e\left(Y_7'\left(Y_8 + \Omega\right) + Y_9 Y_7\right) \tag{24}$$

Subject to the boundary conditions

$$Y_1 = f_w, \quad Y_2 = 1, \quad Y_4 = 1, \quad Y_6 = 1 \text{ and } Y_8 = 1 \quad \text{at } \eta = 0, \tag{25}$$

$$Y_2 = 0, \quad Y_4 = 0, \quad Y_6 = 0 \text{ and } Y_8 = 0 \quad \text{at } \eta \to \infty, \tag{26}$$

where the prime denotes to the differentiation with respect to η. To compute the physical quantities f', θ, ξ and χ. Mathematica package version 9 is used to solve the system of Eqs. (21)–(24) with the boundary conditions (25) and (26).

4 Graphical results and discussion

In this bit of our investigation, we have delineated graphically the impacts of various physical parameters on the velocity, temperature, nanoparticles concentration and density of motile microorganisms on account of suction, injection and impermeable plate surface. Our acquired consequences of velocity and temperature were contrasted with the outcomes in the non-presence of nanoparticles and microorganisms. Likewise, we have displayed graphically the impacts of rising parameters on the fluid motion on account of stretching and shrinking sheet. The effect was exhibited graphically in Figs. 2, 3, 4, 5, 6, 7, 8, 9, 10, 11, 12, 13, 14, 15, 16, 17, 18, 19 and 20.

4.1 Velocity profiles

The impact of various rising parameters on the velocity of the flow has delineated in Figs. 2, 3, 4 and 5. Figure 2 show the impact of non-Newtonian Prandtl parameters A_2 and A_3 on velocity on account of our fluid and on account of missing nanoparticles and microorganisms. By analyzing the graph, it is seen that the velocity is higher without microorganisms and nanoparticles and have a greatest incentive at the wall yet the velocity diminishes persistently to take a minimum value far away from the wall (i.e. $f' \to 0$ *at* $\eta \to \infty$). The influence of suction ($f_w > 0$), injection ($f_w < 0$) and the case of impermeable plate surface ($f_w = 0$) on the velocity distribution is presented in Fig. 3. It is clear that the velocity is greater in the case of injection than in suction.

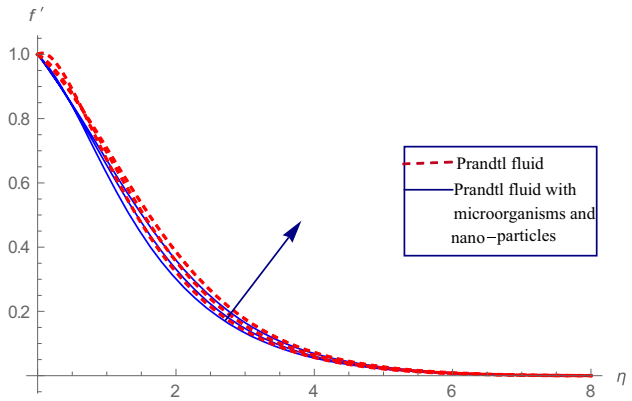

Fig. 2 The velocity of fluid particles f' is plotted against η, for $H_a = L_b = p_e = 1, \epsilon = 0.1, k_r = 0.5, L_e = 5, G_r = 1.5, P_r = 0.7, N_r = N_b = N_t = E_e = \Omega = R_b = .1, f_w = .2, R_n = 0.8. A_2 = A_3 = 0.2, 0.6, 1$

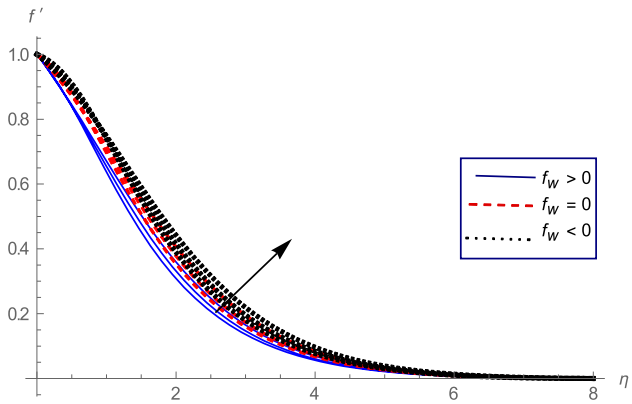

Fig. 3 The velocity of fluid particles f' is plotted against η, for $H_a = L_b = p_e = 1, \epsilon = 0.1, k_r = 0.5, L_e = 5, G_r = 1.5, P_r = 0.7, N_r = N_b = N_t = E_e = \Omega = R_b = .1, f_w = .2, R_n = 0.8. A_2 = A_3 = 0.3, 0.6, 1$

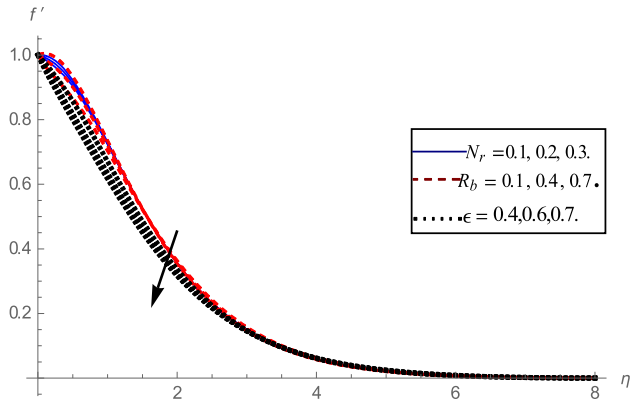

Fig. 4 The velocity of fluid particles f' is plotted against η, for $L_b = H_a = p_e = 1$, $k_r = A_2 = 0.5$, $G_r = 2$, $L_e = 5$, $P_r = 0.7$, $N_b = N_t = E_e = \Omega = 0.1$, $A_3 = 0.5$, $f_w = 0.2$, $R_n = 0.8$

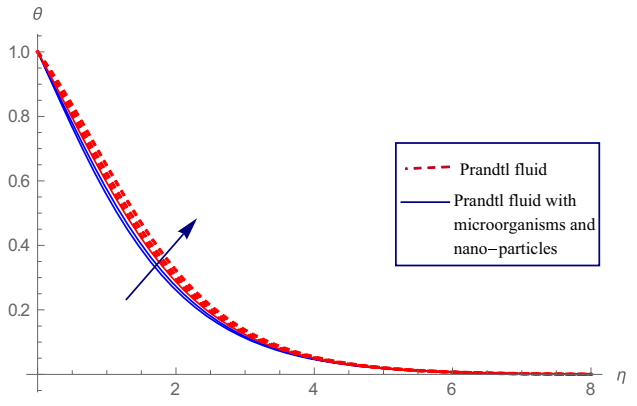

Fig. 7 The temperature of fluid particles θ is plotted against η, for $N_r = N_b = N_t = E_e = \Omega = 0.1$, $P_r = 0.7$, $R_n = 0.8$, $R_b = f_w = 0.2$, $H_a = L_b = p_e = 1$, $\epsilon = 0.1$, $k_r = A_2 = A_3 = 0.5$, $G_r = 2$, $L_e = 5$, $E_c = 0.01, 0.1, 0.2$

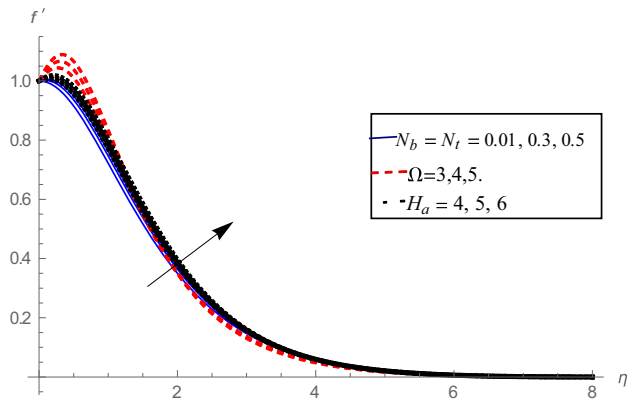

Fig. 5 The velocity of fluid particles f' is plotted against η, for $E_c = N_r = \Omega = 0.1$, $A_3 = 0.5$, $R_b = f_w = 0.2$, $\epsilon = 0.1$, $R_n = 0.8$, $L_b = H_a = p_e = 1$, $k_r = A_2 = 0.5$, $L_e = 5$, $P_r = 0.7$, $G_r = 2$

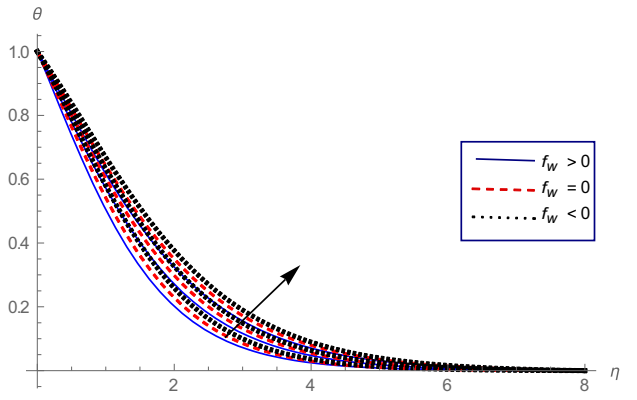

Fig. 8 The temperature of fluid particles θ is plotted against η, for $H_a = L_b = p_e = 1$, $\epsilon = 0.1$, $k_r = 0.5$, $L_e = 5$, $G_r = 2$, $P_r = 0.7$, $N_r = N_b = N_t = E_e = \Omega = R_b = 0.1$, $R_n = 0.8$, $f_w = 0.2$. $P_r = 0.5, 0.7, 1, 2$

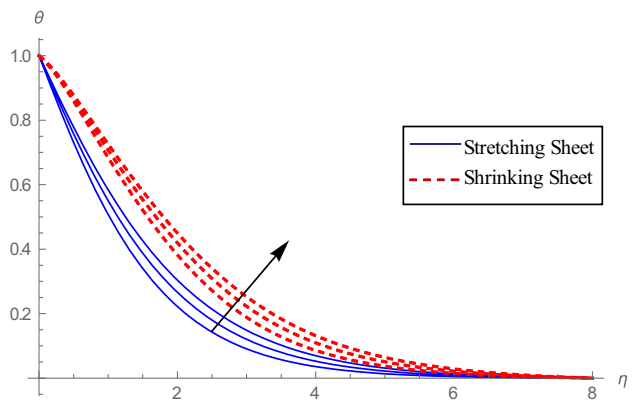

Fig. 6 The temperature of fluid particles θ is plotted against η, for $N_r = N_b = N_t = E_c = E_e = \Omega = 0.1$, $R_b = 0.1$, $f_w = 0.2$, $G_r = 2$, $H_a = L_b = p_e = 1$, $\epsilon = 0.1$, $k_r = A_2 = A_3 = 0.5$, $L_e = 5$, $P_r = 0.7$, $R_n = 1, 1.5, 2$

Figure 4 impact the effect of N_r, R_b and ϵ on velocity, it is noted that, an increase in N_r and R_b imputes the fluid towards the plate surface hence decreasing the boundary layer thickness and the velocity, also since the porous represents an obstacle to flow and therefore, reduced its velocity.

Figure 5 is sketched to visualized the variation in the velocity due to the influence of the Brownian motion parameter N_b, the thermophoresis parameter N_t, the microorganismis concentration difference parameter Ω and the Hartmann number H_a. One is detect that the rising values of N_b and N_t augment the velocity and associated momentum boundary layer thickness, also we see the same behavior for velocity under the effect of Ω and H_a.

4.2 Temperature profiles

The effect of radiation parameter R_n on the temperature for both stretching and shrinking permeable sheet elucidate in Fig. 6. It can be perceived from this figure that the temperature increases for both stretching and shrinking permeable sheet, it takes the maximum value at the boundary layer but constantly decreases far away from the sheet satisfying the boundary conditions (i.e. $\theta \to 0$ at $\eta \to \infty$). Figure 7 is sketched to discuss the effect of E_c on the temperature for both Prandtl fluid and Prandtl fluid with nanoparticles and microorganisms. It is observed that E_c leads to an amplify in the thermal boundary layer thickness and temperature for the two cases but the temperature is higher in the case of the absent of microorganisms and nanoparticles.

Figure 8 is plotted to know the impact of P_r on temperature in the case of suction, injection and impermeable plate surface. An increase in P_r for $f_w > 0$, $f_w = 0$ and $f_w < 0$ lead to increase in the thermal boundary layer thickness and temperature. Figure 9 interpret the effects of the Brownian motion parameter N_b, the thermophoresis parameter N_t and radiation parameter R_n on the temperature distribution. From this plot, we detected that the increase in the values of Brownian motion, thermophoresis and radiation parameter magnifies the temperature and the associated boundary layer thickness. This consistent with the physical concerned that the Brownian motion depend on the unsystematic movement of fluid particles on the surface and the rise of N_b improves this motion of the fluid particles which causes much heat. In addition to this, the increasing values of N_t physically means that the nanoparticles are moving away from the hot permeable surface to the cold which fluid temperature rise.

4.3 Nanoparticle concentration profiles

Figure 10 is sketched to illustrate the features of the traditional Lewis number L_e on the nanoparticles concentration of the fluid for both stretching and shrinking permeable sheet. It can be noted from this graph that the increasing values of L_e decay the concentration of the nanoparticles in the case of stretching sheet, where the Lewis number is inversely proportion to the Brownian diffusion coefficient and so the concentration declines. While the contrary trend is performed for the shrinking sheet. Figure 11 is designed to investigate the impact of the thermophoresis parameter N_t on nanoparticles concentration for suction, injection and impermeable plate surface. It can be seen from this plot that the concentration of the nanoparticles and the associated concentration boundary layer thickness enhance for all cases.

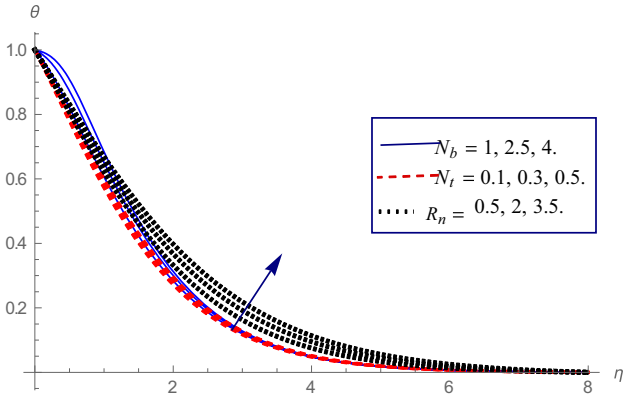

Fig. 9 The temperature of fluid particles θ is plotted against η, for $L_b = H_a = p_e = 1$, $k_r = A_2 = 0.5$, $L_e = 5$, $P_r = 0.7$, $E_c = N_r = \Omega = \epsilon = 0.1$, $A_3 = 0.5$, $G_r = 2$, $R_b = 0.1$, $f_w = 0.2$

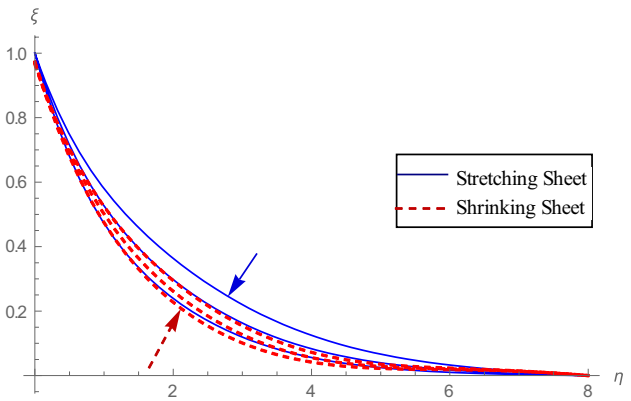

Fig. 10 The nanoparticles concentration of fluid particles ξ is plotted against η, for $L_b = H_a = p_e = 1$, $k_r = A_2 = 0.5$, $L_e = 5$, $P_r = .7$, $E_c = N_r = \Omega = \epsilon = 0.1$, $A_3 = 0.5$, $G_r = 2$, $R_b = 0.1$, $f_w = 0.2$, $L_e = 0.1, 0.3, 0.5$

Figure 12 is devoted to visualized the effect of the Brownian motion N_b, the traditional Lewis number L_e and chemical reaction k_r on the nanoparticles concentration. We can be observed from this sketch that the concentration of the nanoparticles and the associated concentration boundary layer thickness decay for an escalation in N_b. Physically, an extend in the Brownian motion enhances the rate at which the nanoparticles move with different velocities in different random direction so an increase in the unsystematic motion of the fluid leads to decrease in the concentration of the nanoparticles and the associated concentration boundary layer thickness. The same effect occurs for both L_e and k_r .

4.4 Motile microorganisms density profiles

Figures 13, 14 and 15 describe the effects of various parameters on the density of the motile microorganisms. The effect of bioconvection Lewis number L_b on the density of

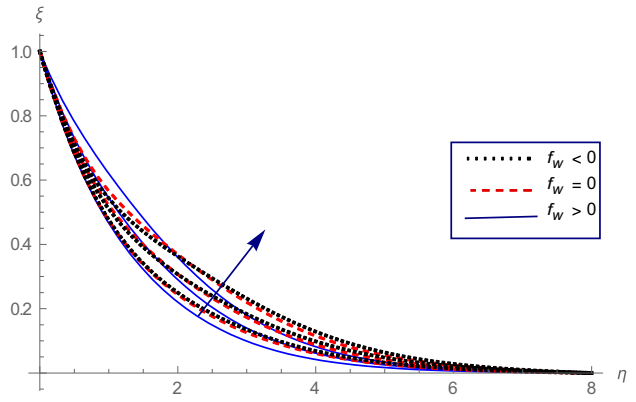

Fig. 11 The nanoparticles concentration of fluid particles ξ is plotted against η, for $H_a = L_b = p_e = 1$, $A_2 = A_3 = k_r = 0.5$, $G_r = 2$, $L_e = 0.5$, $N_r = \epsilon = N_b = E_e = \Omega = 0.1$, $R_b = 0.1$, $R_n = 0.8$, $P_r = 0.7$. $N_t = 0.1, 0.15, 0.2$

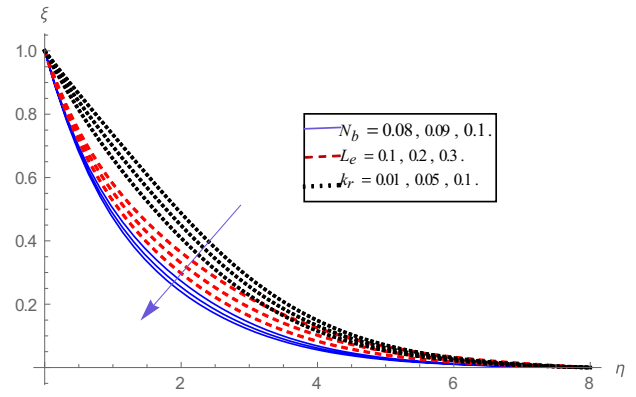

Fig. 12 The nanoparticles concentration of fluid particles ξ is plotted against η, for $L_b = H_a = p_e = 1$, $k_r = A_3 = A_2 = 0.5$, $P_r = 0.7$, $E_c = N_t = \Omega = 0.1$, $R_b = 0.1$, $f_w = 0.2$, $G_r = 2$, $\epsilon = 0.1$

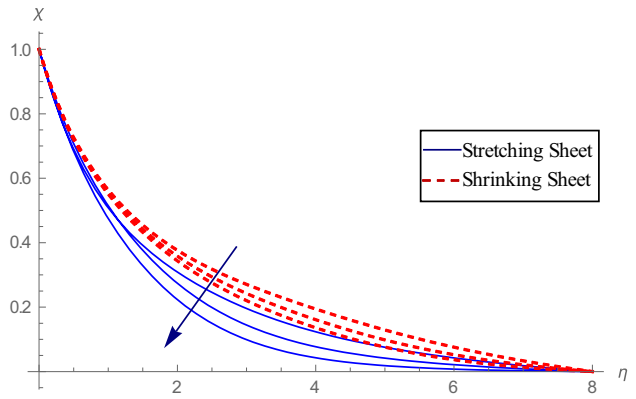

Fig. 13 The nanoparticles concentration of fluid particles χ is plotted against η, for $H_a = 1$, $L_e = p_e = 0.5$, $\epsilon = k_r = 0.5$, $G_r = 2$, $\Omega = 0.6$, $P_r = 0.7$, $N_r = E_c = N_b = N_t = \epsilon = R_b = 0.1$, $A_2 = A_3 = 1.5$, $f_w = 0.2$. $L_b = 0.1, 0.18, 0.25$

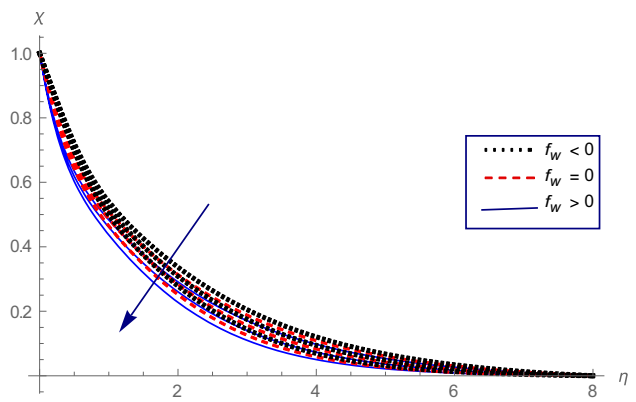

Fig. 14 The nanoparticles concentration of fluid particles χ is plotted against η, for $H_a = p_e = 1$, $L_e = 5$, $\epsilon = 0.1$, $k_r = 0.3$, $A_2 = A_3 = 0.5$, $L_b = 0.3$, $N_r = N_b = N_t = E_e = \Omega = R_b = 0.1$, $G_r = 2$, $P_r = 0.7$. $R_n = 0.1, 1, 3$

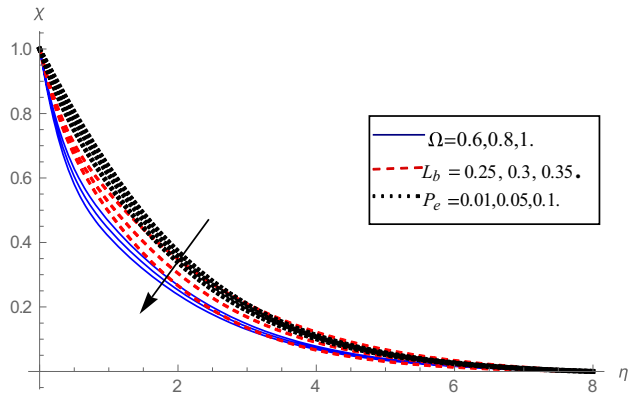

Fig. 15 The nanoparticles concentration of fluid particles χ is plotted against η, for $H_a = 1$, $k_r = 0.5$, $\epsilon = 0.1$, $A_2 = A_3 = 0.5$, $P_r = 0.7$, $G_r = 2$, $L_e = 5$, $N_b = N_t = E_c = \epsilon = N_r = R_b = 0.1$, $R_n = 0.8$, $f_w = 0.2$

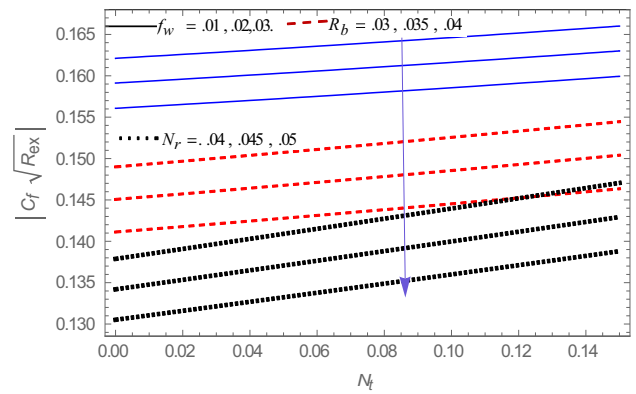

Fig. 16 The local skin friction of fluid particles $\left|\sqrt{R_{ex}}C_f\right|$ is plotted against N_t, for $k_r = A_3 = A_2 = 0.5$, $G_r = 2$, $L_e = 5$, $P_r = 0.7$, $E_e = \Omega = 0.1$, $R_n = 0.8$, $N_b = N_t = 0.1$, $L_b = H_a = p_e = 1$

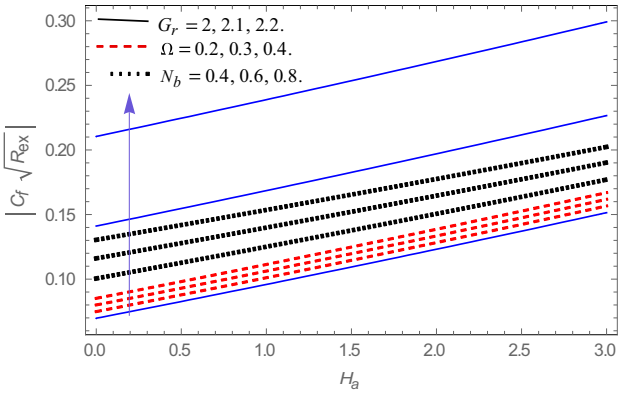

Fig. 17 The local skin friction of fluid particles $\left|\sqrt{R_{ex}}C_f\right|$ is plotted against H_a, for $L_b = p_e = 1$, $k_r = A_3 = A_2 = 0.5$, $L_e = 5$, $P_r = 0.7$, $R_n = 0.8$, $E_c = N_r = N_t = 0.1$, $R_b = 0.1$, $f_w = 0.2$

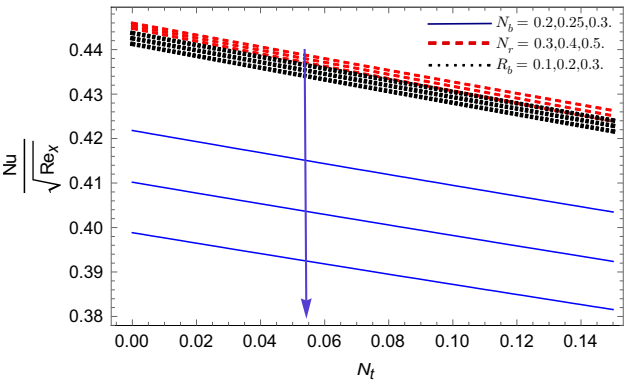

Fig. 18 The local Nusselt number of fluid particles $\frac{Nu}{\sqrt{Re_x}}$ is plotted against N_t, for $L_b = H_a = p_e = 1$, $k_r = \epsilon = A_2 = 0.5$, $G_r = 2$, $L_e = 5$, $N_t = E_c = \Omega = 0.1$, $A_3 = 0.5$, $P_r = 0.7$, $R_n = 0.8$

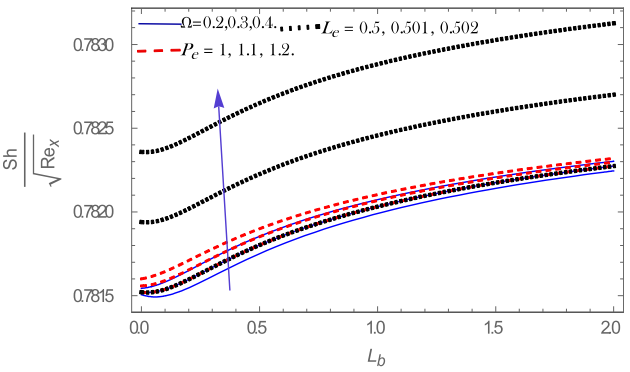

Fig. 19 The local Sherwood number of fluid particles $\frac{Sh}{\sqrt{Re_x}}$ is plotted against L_b, for $H_a = 1$, $k_r = \epsilon = A_2 = 0.5$, $G_r = 2$, $N_t = E_e = 0.1$, $A_3 = 0.5$, $P_r = 0.7$, $R_n = 0.8$, $R_b = 0.1$, $f_w = 0.2$

the motile microorganisms of the fluid for both stretching and shrinking permeable sheet can be seen from Fig. 13. The boosting the values of L_b decay the density

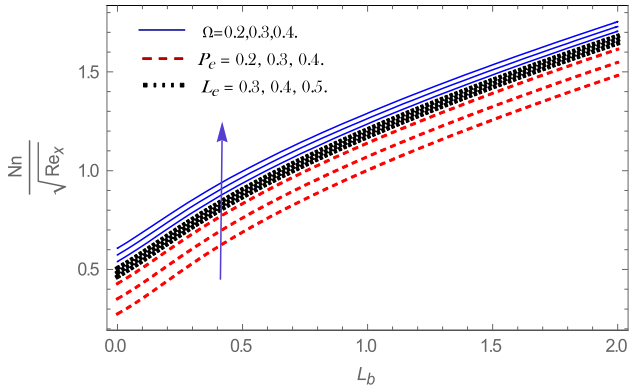

Fig. 20 The density number of the motile microorganisms of fluid particles $\frac{Nn}{\sqrt{Re_x}}$ is plotted against L_b, for $H_a = 1$, $k_r = \epsilon = A_2 = 0.5$, $G_r = 2$, $N_t = E_e = 0.1$, $A_3 = 0.5$, $P_r = 0.7$, $R_n = 0.8$, $R_b = 0.1$, $f_w = 0.2$

of the motile microorganisms and the associated thickness of density of the motile microorganisms in the case of stretching and shrinking sheet. Figure 14 is sketched to interpret the variations in the density of the motile microorganisms under the influence of the radiation parameter R_n for suction, injection and impermeable plate surface. It is noted that an enlarge in R_n leads to decrease in the density of the motile microorganisms and the associated thickness. Figure 15 is plotted to know the impact of the microorganismis concentration difference parameter Ω, bioconvection Lewis number L_b and bioconvection Peclet number P_e on the density of the motile microorganisms. From this plot, one can detect that the rising values of the microorganismis concentration difference parameter, the bioconvection Lewis number and bioconvection Peclet number decline the density of the motile microorganisms and the associated thickness.

4.5 Effects of parameter variations on C_{fx},Nu_x, Sh_x, Nn_x

The impacts of the physical parameters on the dimensionless local skin friction is sketched in Figs. 16 and 17. It is observed that an escalating in f_w, R_b and N_r decline the local skin fraction, while the reverse effects are observed with enlarging G_r, Ω and N_b. Figure 18 is elucidate the impact of N_b, N_r and R_b on the local Nusselt number, we detected that the boosting values of N_b, N_r and R_b downturned the rate of heat transfer.

Figure 19 is devoted to investigate the fluctuations in the local Sherwood number for various values of Ω, P_e and L_e. From this graph, it is noted that as we enlarged the values of Ω, P_e and L_e the local Sherwood number augmented. Figure 20 is plotted to discuss the effects of Ω, P_e and L_e on the density number of the motile

Table 1 Comparison for numerical values of (a) $f'(1)$ with Mutuku and Makinde [12] for distinct values of Hartmann number when $A_2 = 1, A_3 = \varepsilon_1 = R_n = K_r = 0, N_b = N_t = N_r = R_b = E_c = 0.1, P_r = 0.7, G_r = P_e = L_b = 1, L_e = 5$ and (b) $\theta(1)$ with Mutuku and Makinde [12] for distinct values of Hartmann number when $A_2 = 1, A_3 = \varepsilon_1 = R_n = K_r = 0, N_b = N_t = N_r = R_b = E_c = 0.1, P_r = 0.7, G_r = P_e = L_b = 1, L_e = 5$

H_a	Mutuku and Makinde [12]	Present
(a)		
1	0.392063	0.392063
1.5	0.343884	0.343884
2	0.304787	0.304787
(b)		
1	0.541643	0.541643
1.5	0.559666	0.559666
2	0.574690	0.574690

microorganisms. It observed that increasing the values of Ω, P_e and L_e lead to enhance the density number of the motile microorganisms.

5 Validation of results

Equations (10)–(15) p. 90 of Mutuku and Makinde [12] were solved in the same way as in my paper, which it is considered as special case of my paper when $A_2 = 1, A_3 = \varepsilon_1 = R_n = K_r = 0$. Thus the comparisons were made for velocity and temperature through Table 1a, b and Fig. 21a, b.

6 Conclusions

In this present investigation, bioconvection of Prandtl nanofluid involving gyrotactic microorganisms for both stretching and shrinking sheet in the instances of suction ($f_w > 0$), injection ($f_w < 0$) and impermeable plate surface ($f_w = 0$) in conjunction of magnetic field, radiation and chemical reaction has been conducted and analyzed. Our system of equations are solved numerically by using Rung–Kutta–Merson method with Newton iteration in a shooting and matching technique. It is firmly accepted that the results of this problem are of great interest for antimicrobial application of nanotechnology, the necessity for novel antibiotics comes from the relatively high incidence of bacterial infection and developing resistance of bacteria to conventional antibiotics, so new techniques for decreasing bacterial movement which are nanotechnology that is of extraordinary enthusiasm as a way to deal with executing or lessening the action of various microorganisms has made by Siel et al. [20]. Based on the numerical results, some of the interesting observations are exposed as follows:

1. A correlation between arrangements of our fluid motion and on account of the missing of nanoparticles and microorganisms has been made under the impacts of Prandtl parameters and Eckert number. From this correlation, we noticed that the velocity profile and temperature profile are higher than that in the missing of nanoparticles and microorganisms.
2. The impacts of rising parameters on temperature, nanoparticles concentration and density of motile microorganisms with respect to the stretching and shrink-

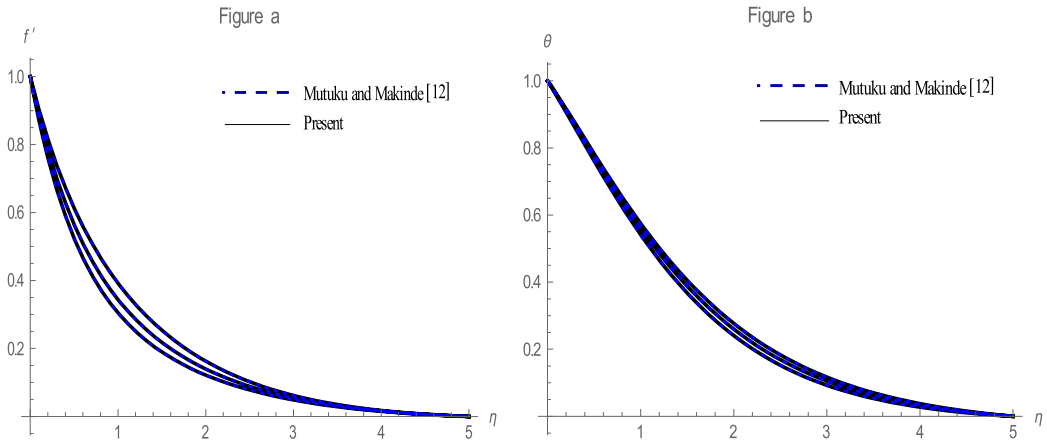

Fig. 21 Comparison for numerical values of f' and θ with Mutuku and Makinde [12] for distinct values of Hartmann number when $A_2 = 1, A_3 = \varepsilon_1 = R_n = K_r = 0, N_b = N_t = N_r = R_b = E_c = 0.1, P_r = 0.7, G_r = P_e = L_b = 1, L_e = 5$

ing sheet have been talked about. Unmistakably the temperature and density of motile microorganisms are higher on account of shrinking sheet than the instance of stretching sheet.

3. Analyzing the impact of various parameters on velocity, temperature, nanoparticles concentration and density of motile microorganisms for suction ($f_w > 0$), injection ($f_w < 0$) and the case of impermeable plate surface ($f_w = 0$). It is worth mentioning that the velocity, temperature, nanoparticles concentration and density of motile microorganisms are higher for injection and lower in suction but in between the two cases for impermeable plate surface.
4. The local skin friction, local Nusselt number, local Sherwood number and the density number of the motile microorganisms are strongly affected by Grashof number, buoyancy ratio parameter, bioconvection Rayleigh number and microorganism is concentration difference parameter.

Compliance with ethical standards

Conflict of interest The authors declare that they have no conflict of interest.

References

1. Tausif S et al (2016) Multiple slip effects on bioconvection of nanofluid flow containing gyrotactic microorganisms and nanoparticles. J Mol Liq 220:518–526
2. Das K et al (2015) Nanofluid bioconvection in presence of gyrotactic microorganisms and chemical reaction in a porous medium. J Mech Sci Technol 29(11):4841–4849
3. Bhatti MM et al (2019) Numerical study of heat transfer and Hall current impact on peristaltic propulsion of particle-fluid suspension with compliant wall properties. Mod Phys Lett B 33:1950439
4. Waqas H et al (2019) Thermally developed Falkner-Skan bioconvection flow of a magnetized nanofluid in the presence of a motile gyrotactic microorganism: Buongiorno's nanofluid model. Phys Scr 94:115304
5. Marin M et al (2019) On the partition of energies for the backward in time problem of thermoelastic materials with a dipolar structure. Symmetry 11:863
6. Waqas H et al (2019) Analysis on the bioconvection flow of modified second-grade nanofluid containing gyrotactic microorganisms and nanoparticles. J Mol Liq 291:111231
7. Sarkar A et al (2016) On the onset of bioconvection in nanofluid containing gyrotactic microorganisms and nanoparticles saturating a non-Darcian porous medium. J Mol Liq 223:725–733
8. Khan NS et al (2017) Mixed convection in gravity-driven thin film non-Newtonian nanofluids flow with gyrotactic microorganisms. Result in Physics 7:4033–4049
9. Khan M et al (2017) Impact of nonlinear thermal radiation and gyrotactic microorganisms on the Magneto-Burgers nanofluid. Int J Mech Sci 130:375–382
10. Mahdy A (2017) Gyrotactic microorganisms mixed convection nanofluid flow along an isothermal vertical wedge in porous media. World Academy of Science, Engineering and Technology International Journal of Aerospace and Mechanical Engineering 11(4):840–850
11. Raju CSK et al (2017) Flow of Casson fluid over a moving wedge filled with gyrotactic microorganisms. Advanced Power Technology 28:575–583
12. Mutuku WN, Makinde OD (2014) Hydromagnetic bioconvection of nanofluid over a permeable vertical plate due to gyrotactic microorganisms. Comput Fluids 95:88–97
13. Alsaedi A et al (2017) Magnetohydrodynamic (MHD) stratified bioconvective flow of nanofluid due to gyrotactic microorganisms. Advanced Power Technology 28:288–298
14. Mekheimer KS et al (2013) Peristaltically flow due to a surface acoustic wavy moving wall. Chinese Journal of Physics 51(5):954–968
15. Ramzan M et al (2017) Radiative magnetohydrodynamic nanofluid flow due to gyrotactic microorganisms with chemical reaction and non-linear thermal radiation. Int J Mech Sci 130:31–40
16. Eldabe NT, Ramadan SF (2018) Effects of wall properties, heat absorption and chemical reaction on peristaltic motion of Rivlin–Ericksen fluid through porous medium in vertical channel. Applied Mathematics & Information Sciences Letters 6(3):99–106
17. Mekheimer KS et al (2014) Peristaltically induced MHD slip flow in a porous medium due to a surface acoustic wavy wall. Journal of the Egyptian Mathematical Society 22(1):143–151
18. Akbar NS et al (2012) Peristaltic flow of a Prandtl fluid model in an asymmetric channel. International Journal of the Physical Sciences 7(5):687–695
19. Zaman S, Gul M (2019) Magnetohydrodynamic bioconvective flow of Williamson nanofluid containing gyrotactic microorganisms subjected to thermal radiation and Newtonian conditions. J Theor Biol 479:22–28
20. Seil JT, Webster TJ (2012) Antimicrobial applications of nanotechnology: methods and literature. International Journal Nanomedicine 7:2767–2781